

Atomic Structure of Si-Rich 6H-SiC(000 $\bar{1}$)-2×2 Surface

Y. Hoshino^{1,3*}, R. Fukuyama¹, Y. Matsubara¹, T. Nishimura¹, S. Tanaka²,
M. Kohyama², and Y. Kido¹

Abstract

The atomic structure of the Si-rich 6H-SiC(000 $\bar{1}$)-2×2 surface has been determined by high-resolution medium energy ion scattering (MEIS) and photoelectron spectroscopy using synchrotron-radiation-light (SR-PES). The MEIS analysis reveals the fact that Si adatoms (0.2-0.3 ML) overlie a Si-adlayer (0.8-0.9 ML) sitting on the bulk-truncated surface (1ML=1.22×10¹⁵ atoms/cm²). In fact, we observed two surface-related components in the Si 2p core level spectra corresponding to the adatom and the adlayer Si atoms and the intensity ratio of the former to the latter was ~1/3. On the other hand, the C 1s core level observed has the bulk component only. We propose an adatom-adlayer model satisfying the 2×2 surface reconstruction, three-fold symmetry and the results obtained by MEIS and SR-PES. Further MEIS analysis using focusing/blocking effect clearly shows that the Si-adatoms take an H-site. The surface structure predicted by the *ab initio* molecular dynamics calculation coincides with the above structure model except for slight lateral displacements of the Si-adlayer and reproduces well the present experimental results of MEIS and SR-PES.

¹ Dept Physical Sciences, Faculty of Science. and Engineering, Ritsumeikan University, Kusatsu, Shiga 525-8577

² National Institute of Advanced Industrial Sci. and Technol, Ikeda, Osaka 563-8577

³ Dept. Electronic Sci. and Eng., Kyoto University, Nishikyo-ku, Kyoto 610-8510

I. INTRODUCTION

Silicon carbide has attracted much attention as the best candidates for high temperature, high power and high frequency electronic devices. In the device fabrication, the atomic structure of crystal surfaces influences the quality of epitaxial layers and the reaction processes with various gases and metal films. So far, a lot of investigations[1-5] have been done for the Si-terminated (0001) surfaces mainly from practical aspect of its low interfacial defect densities and good quality of the epilayers. In contrast, we have only a few reports on the C-terminated ($000\bar{1}$) surfaces because of its large defect levels at oxide/semiconductor interfaces and difficulties in controlling dopant concentrations. Recently, Fukuda et al.[6] succeeded in considerable reduction of the interfacial levels by a pyrogenic oxidation followed by annealing under hydrogen ambient. In addition, the oxidation rate for the C-terminated SiC surface is much larger than that for the Si-terminated one. Therefore, now it is strongly required to characterize the oxidation and the metal/SiC contact formation for the C-terminated surface.

It is known that the SiC($000\bar{1}$) surface takes several surface reconstructions dependent on sample preparation. Bernhardt et al. reported that a (3×3) surface reconstruction appeared by heating at 1050°C for 15 min in an ultra-high vacuum (UHV) and prolonged heating at 1075°C led to a Si-depleted 2×2 surface ($[2\times 2]_C$)[7,8]. These two phases tend to coexist presumably due to nearly equal surface energies of the two structures. Scanning tunneling microscope (STM) and quantitative low energy electron diffraction (LEED) analyses showed that the $[2\times 2]_C$ surface consisted of Si adatoms of 0.25 ML (1 ML = 1.22×10^{15} atoms/cm²) taking an H₃-site. Heating at temperatures above 1150°C led to a (1×1) graphitized surface. On the other hand, annealing at 1150°C in Si-flux of about 1 ML/min for 20 min formed a Si-enriched Si($000\bar{1}$)-2×2 surface ($[2\times 2]_{Si}$). Johansson et al.[9] also prepared the 3×3 reconstructed surface by heating at 1050°C and concluded from C 1s core level analysis that the surface consisted of at least two carbon overlayers.

In this work, we first prepared the Si-enriched SiC($000\bar{1}$)-2×2 surface by heating at 950°C

for 5 min in UHV after pre-deposition of Si (3 ML). It is shown that this 2×2 surface is the Si-enriched $[2\times 2]_{\text{Si}}$ surface whose existence was first reported by Bernhardt et al.[7,8]. Unfortunately, however, the surface structure has not been clarified yet. High-resolution medium energy ion scattering (MEIS) combined with photoelectron spectroscopy using synchrotron-radiation-light (SR-PES) is a powerful tool to determine the atomic configuration of surfaces and interfaces. The structural analysis was carried out *in situ* at the beamline named SORIS allowing both MEIS and SR-PES. We also performed the *ab initio* calculations based on the density-functional theory (DFT) using the pseudopotential method. Finally, an energetically stable and most probable surface structure satisfying the experimental results is proposed.

II. EXPERIMENT

We purchased N-doped 6H-SiC(000 $\bar{1}$) wafers from CREE Inc. and cut them into small pieces with a typical size of 10×10 mm². After cleaning the surface by a modified RCA method[10], the sample was introduced into an UHV chamber and degassed at 600°C for 5 h. Then cooling it down to room temperature (RT), a small amount of Si (3 ML) was deposited by molecular beam epitaxy (MBE) and after that the sample was annealed at 950°C for 5 min. Reflection high-energy electron diffraction (RHEED) showed a sharp 2×2 pattern with strong Kikuchi lines. This surface is stable without coexistence of other surface phases.

The experiment was performed at beam line 8 constructed at Ritsumeikan SR Center, which combined MEIS with SR-PES. All the systems were working under UHV conditions. The samples were heated by infrared-radiation and the temperature was monitored with a Pt-Rh thermocouple set about 1mm above the sample. A well collimated He⁺ beam was incident on a sample and backscattered He⁺ ions were detected by a toroidal electrostatic analyzer (ESA) with an excellent energy resolution ($\Delta E/E$) of 9.0×10^{-4} . On the other hand, emitted photoelectrons were analyzed by a hemispherical ESA with an energy resolution of about 10 meV at a typical pass energy of 2.95 eV. The total energy resolution was estimated

to be 100-150 meV including contributions from a Doppler broadening and energy spreads of incident photons. The details of the experimental setup are described in the previous reports[11,12]. The present MEIS analysis determined the elemental depth profiles and the atomic configuration using the ion blocking and focusing effects. Complementally, the information on the chemical bonding and the electronic structure was obtained by SR-PES analysis.

It must be noted that the toroidal ESA detected only He^+ ions. In order to determine the absolute amount of atoms of interest, we need the scattered He^+ fractions as a function of scattered He^+ velocity. For He ions scattered from low Z atoms ($Z < \sim 20$) located near a top-surface, the He^+ fraction does not reach an equilibrium[13]. So we measured in advance the surface peaks for amorphous-Si and graphite targets and obtained the He^+ fractions, which was enhanced by 120 % and 200 %, respectively compared with the equilibrium He^+ fractions which were derived from the scattering yields from the deeper layers.

III. *AB INITIO* CALCULATIONS

The *ab initio* molecular dynamics (MD) calculations were performed by the *ab initio* pseudopotential method based on the DFT within the local density approximation[14]. The Norm-conserved pseudopotentials developed by Troullier-Martins[15] were employed. In order to get the electronic ground state, we used the residual minimization method and direct inversion in the iterative subspace (RMM-DIIS)[16,17] and the conjugate-gradient method¹⁸ coupled with the efficient charge-mixing scheme[19,20]. Here, a plane-wave cutoff energy of 40 Ry was selected based on the tests of total energy convergence. We developed an appropriate supercell of a $6\text{H-SiC}(000\bar{1})-2\times 2$ surface. The supercell consists of a Si-atom, three Si-adlayer atoms, six C-Si bilayers with a surface C layer, four hydrogen atoms for termination of dangling bond of the backside surface C atoms. In addition, the supercell includes six vacuum layers, which sufficiently separates each 2×2 surface slab. Three and six sampling k-points for self-consistent calculations were used. Thus we obtain

stable atomic configurations through relaxation processes according to Hellmann- Feynman forces, which converged within 0.001 eV/Å per each atom. The bottom C-Si bilayer was fixed in the bulk configuration of the theoretical lattice constants ($a=3.08$ Å, $c=15.08$ Å). The present scheme was successfully applied previously to adhesive energies and Schottky barrier-heights of 3C-SiC/Ti interfaces[21,21] and 3C-SiC/Al interfaces[23,24].

IV. RESULTS AND DISCUSSION

Figure 1 shows the MEIS spectrum observed for 120 keV He^+ ions incident at 54.7° and scattered to 85.1° in the $(11\bar{2}0)$ plane with respect to surface normal. Such a grazing emergence geometry makes it possible to improve the depth resolution and thus to separate the scattering components from each atomic layer. The surface peak from Si consists of two components, from a Si-adlayer and the top C-Si bi-layer. The C front edge shifts by ~ 1 keV to the lower energy side, indicating the existence of a Si-adlayer of about 1 ML on the top C-Si bilayer. The absolute amount of the Si-adlayer is derived to be 1.1 ± 0.1 ML from the area of the deconvoluted surface peak and from the knowledge of the integrated beam current, the solid angle subtended by the toroidal ESA, and the He^+ fraction. Taking a further glancing emergent geometry (88.0°) clearly resolves the previous Si-adlayer into two scattering components, Si-adatoms of ~ 0.25 ML and an underlying Si-adlayer of ~ 0.95 ML (see Fig. 2).

Figure 3 shows the Si 2p core level spectra observed for incident photon energy of 140 and 280 eV at emission angles of 0° and 60° with respect to surface normal. The spectra are decomposed into three components, bulk and two surface-related (S1 and S2) ones, assuming Gaussian shapes, the singlet/triplet branching ratio of 1/2 and the energy interval of 0.60 eV. From the bottom to top, the spectra are more surface sensitive. The binding energy of the bulk component measured from the Fermi level was determined precisely by taking higher photon energy of 280 and 420 eV which gives a larger escape depth. The surface-related components denoted by S1 and S2 have lower binding energies of -1.21 ± 0.1 and -0.41 ± 0.1

eV, respectively relative to that of the bulk. From the relative intensity ratios dependent on photon energy and emission angle, the components S1 and S2 are assigned to the Si-adatoms and the Si-adlayer, respectively. The intensity ratio of S1/S2 at normal emission is estimated to be about 1/3. This is consistent with the previous MEIS result. We also observed the C 1s spectra at photon energy of 420 eV and found the bulk component only. This also supports the surface structure taking Si-adatoms on a Si-adlayer overlying the top C-Si bilayer.

Now we propose a probable surface structure satisfying the above MEIS and PES results considering the 2×2 reconstruction with three fold symmetry, as shown in Fig. 4. The shaded area indicates the 2×2 unit cell. In this model, three Si atoms of the Si-adlayer making a trimer bonded to one Si-adatom and the amounts of the Si adatoms and Si-adlayer are 0.25 and 0.75 ML, respectively. There are two possibilities concerning the location of the Si adatoms, a T-site (left side of Fig. 4) or an H-site (right side of Fig. 4). In Fig. 4, the adatom S is located at the center of the triangle PQR of the adlayer in the T-site model, and is located at the center of the triangle PQ'R' in the H-site model. Note that the adlayer atoms P, Q, R, Q' and R' are common in both the models. According to this model, the amount of 0.25 ML of C atoms of the top C-Si bilayer is visible from the surface normal direction. To confirm this situation, we measured the MEIS spectrum at normal incidence. As a result, it was found that almost C atoms of the top C-Si bilayer are visible from the normal direction. This suggests a significant lateral distortion of the Si-adlayer.

Considering the above structural model and the C_{3v} symmetry, we performed the *ab initio* MD calculations. We determined the atomic configurations minimizing the total energy for three specific terminations of the stacking sequence, i.e., S-1(CACBAB), S-2(BCACBA) and S-3(ABCACB) against the bulk stacking sequence ABCACB of 6H-SiC²⁵. The most stable surface structure is shown in Fig. 5. The surface structure does not depend on the termination of the stacking sequence as previous calculation of silicate adlayers on $\sqrt{3}\times\sqrt{3}$ surface[25], and no significant preference is seen for H- or T-site of the Si-adatoms. The

Si-adlayer consists of two types of trimers, PQR and PQ'R' in Fig. 5, holding C_{3v} symmetry and the larger one (PQ'R') is bonded to one Si adatom (S in Fig. 5, where Si-adatoms take an H-site). The presence of the two types of trimers on the Si-adlayer means the lateral displacement of each Si atom above the C atom, which is consistent with the MEIS experiment. It is interesting that the triangular bonding of Si occurs stably at the smaller trimer (PQR) with enough bond charges. In contrast, the Si-adatoms take a perfectly symmetric position with respect to the bulk crystal structure.

The bond length between the adlayer Si atom and the C atom is 1.88 Å, which is close to the bulk SiC bond length, 1.87 Å in theoretical calculations and 1.89 Å in experiments. The interlayer distance between the Si-adlayer and the top C-Si bilayer is slightly smaller than this Si-C bond length, because of the lateral displacement of each Si-adlayer atom, 0.35 Å, as shown in Fig. 5. The bond length between the adlayer Si atoms is 2.48 Å, which is slightly larger than that of 2.41 Å between the adlayer Si atom and the Si-adatom. These bond lengths are larger than the bulk Si bond length of 2.33 Å in theoretical calculations and 2.35 Å in experiments. The angle between the two adatom-adlayer bonds is 99.7°, which is about 9 % smaller than the tetrahedral angle of the bulk Si. The origin of this distortion may have some relation with the electronic structure of the dangling bond of the adatom.

In any case, the present structure minimizes the number of dangling bonds and also minimizes the total energy, although there exist bond length and bond angle distortions associated with peculiar bonding network. There remain two kinds of dangling bonds at the top C-Si bilayer and the Si-adatom, which should cause some surface electronic states. Experimentally, we have recently observed the valence band spectra and found non-dispersive two surface states with energies of 1.5 and 2.2 eV below the Fermi level probably originating from the dangling bonds of the Si adatoms and of the top C-Si bilayer visible from the normal direction[26]. The detailed theoretical and experimental results of the electronic structure will be given in the near future.

In order to determine whether the Si-adatoms take the H-site or T-site, we performed an

azimuth scan for the scattering component from Si of the top C-Si bilayer at fixed incident and emergent angles of 54.7° and 85.1° , respectively. Such a grazing-angle emission condition enhances the focusing and blocking effects due to the contribution from a large number of atoms lying in a string not from a single atom only. If the Si-adatoms take an H-site, the He ions scattered from Si of the top C-Si bilayer would undergo a pronounced focusing effect at the $[11\bar{2}0]$ -azimuth (see Fig. 4). On the other hand, a T-site location gives a blocking effect in this scattering geometry. At the $[1\bar{1}00]$ -azimuth, both H- and T-sites block the He ions scattered from Si of the top C-Si bilayer and lead to reduction of the scattering yield. Figure 6 shows the observed azimuth scan profile for the scattering component mainly from Si of the top C-Si bilayer. Here, 0° and 30° correspond to the $[1\bar{1}00]$ - and $[11\bar{2}0]$ -azimuth angle, respectively. We also performed Monte Carlo simulations of ion trajectories assuming the atomic configurations predicted by the *ab initio* calculations. Apparently, the observed profile has a pronounced focusing effect at the $[11\bar{2}0]$ -azimuth and thus supports the H-site location of the Si-adatoms.

V. CONCLUSION

The $6\text{H-SiC}(000\bar{1})\text{-}2\times 2$ surface was prepared by heating at 950°C in UHV after Si deposition of 3 ML. This surface corresponds to just the Si-rich $[2\times 2]$ surface ($[2\times 2]_{\text{Si}}$) which was first reported by Bernhardt et al.[7,8]. Our high-resolution MEIS and SR-PES analyses have revealed the fact that there exist the Si-adatoms ($\sim 1/3$ ML) on the Si-adlayer ($\sim 0.8\text{-}0.9$ ML) sitting on the top C-Si bilayer. The present MEIS and PES results predict the surface structure consisting of the Si-adlayer which forms hexagons in the unit of a trimer bonded to a Si-adatom (H- or T-site). However, the amount of the C atoms visible from the normal direction was significantly larger than that expected from the above structure model, suggesting a slight lateral distortion of the Si-adlayer. So, we performed the *ab initio* MD calculations using the plane waves as a basis function and employing the pseudopotential method. The surface atomic configuration minimizing the total energy basically supports the Si-adatom/Si-adlayer model but the bonding between the Si-trimer and Si-adatom is

symmetrically elongated in the lateral plane. This structure model explains completely the MEIS and SR-PES results. However, there are no significant differences between the total energies and also the structures of the Si-adlayer calculated assuming the H- and T-site location of the Si-adatoms. The azimuth scan for the scattering component from Si of the top C-Si bilayer under a grazing emission condition clearly shows preference of the H-site location.

ACKNOWLEDGEMENTS

The authors would like to thank Prof. H. Namba and Dr. K. Ogawa for maintaining the SR-PES system of BL-8 at Ritsumeikan SR Center. Special thanks are also due to Dr. T. Okazawa for his help in the MEIS experiment.

References

- [1] J. R. Waldrop, *J. Appl. Phys.* **75**, 4548 (1994).
- [2] L. I. Johansson, F. Owman, and P. Mårtensson, *Phys. Rev. B* **53**, 13793 (1996).
- [3] H. Matsunami and T. Kimoto, *Mater. Sci. Eng., R.* **20**, 125 (1997).
- [4] Y. Hoshino, T. Nishimura, T. Yoneda, K. Ogawa, H. Namba, and Y. Kido, *Surf. Sci.* **505**, 234 (2002).
- [5] Y. Hoshino, S. Matsumoto, and Y. Kido, *Phys. Rev.* **B 69**, 155303 (2004).
- [6] K. Fukuda, S. Suzuki, T. Tanaka, and K. Arai, *Appl. Phys. Lett.* **76**, 1585 (2000).
- [7] J. Bernhardt, M. Nerdling, U. Starke, and K. Heinz, *Mater. Sci. Eng.*, **B 61**, 207 (1999).
- [8] J. Bernhardt, A. Seubert, M. Nerdling, U. Starke, and K. Heinz, *Mater. Sci. Forum*, **338-342**, 345 (2000).
- [9] L.I. Johansson, P.-A. Glans, N. Hellgren, *Surf. Sci.* **405**, 288 (1998).
- [10] W. Kern and D.A. Poutinen, *RCA Rev.* **31**, 187 (1970).
- [11] Y. Kido, H. Namba, T. Nishimura, A. Ikeda, Y. Yan, and A. Yagishita, *Nucl. Instrum. Methods Phys. Res.* **B 135-138**, 798 (1998).

- [12] T. Nishimura, A. Ikeda, and Y. Kido, *Rev. Sci. Instrum.* **69**, 1671 (1998).
- [13] Y. Kido, T. Nishimura, and F. Fukumura, *Phys. Rev. Lett.* **82**, 3352 (1999).
- [14] J. P. Perdew and A. Zunger, *Phys. Rev. B* **23**, 5048 (1981).
- [15] N. Troullier and J. L. Martins, *Phys. Rev. B* **43**, 1993 (1991).
- [16] P. Pulay, *Chem. Phys. Lett.* **73**, 393 (1980).
- [17] G. Kresse and J. Furthmüller, *Phys. Rev. B* **54**, 11169 (1996).
- [18] D. M. Bylander, L. Kleinman and S. Lee, *Phys. Rev. B* **42**, 4021 (1990).
- [19] P. Pulay: *J. Comp. Chem.* **3**, 556 (1982).
- [20] G. P. Kerker: *Phys. Rev. B* **23**, 3082 (1981).
- [21] S. Tanaka and M. Kohyama, *Phys. Rev. B* **64**, 235308 (2001).
- [22] M. Kohyama and J. Hoekstra, *Phys. Rev. B* **61**, 2672 (2000).
- [23] S. Tanaka and M. Kohyama, *Appl. Surf. Sci.* **216**, 471 (2003).
- [24] J. Hoekstra and M. Kohyama, *Phys. Rev. B* **57**, 2334 (1998).
- [25] W. Lu, P. Krüger and J. Pollmann, *Phys. Rev. B* **61**, 13737 (2000).
- [26] Y. Hoshino, R. Fukuyama and Y. Kido, *Phys. Rev. B* **70**, 165303 (2004).

Figure Captions

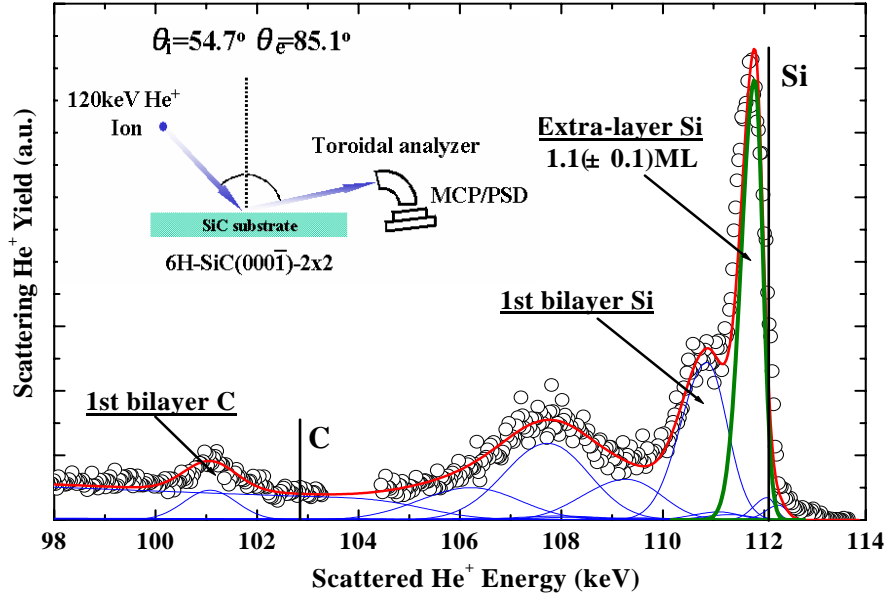


FIG.1. MEIS spectrum observed for 120keV He^+ ions incident on the $6\text{H-SiC}(000\bar{1})-2\times 2$ surface at an angle of 54.7° and scattered to 85.1° in the $(11\bar{2}0)$ plane. Open circles indicate the observed spectrum and the solid curves are the best-fitted ones (bold: total, light: deconvoluted) assuming a Si-adlayer of 1.1 ML sitting on the top C-Si bilayer. The bold and thin curves correspond to total and the scattering component from each atomic layer, respectively.

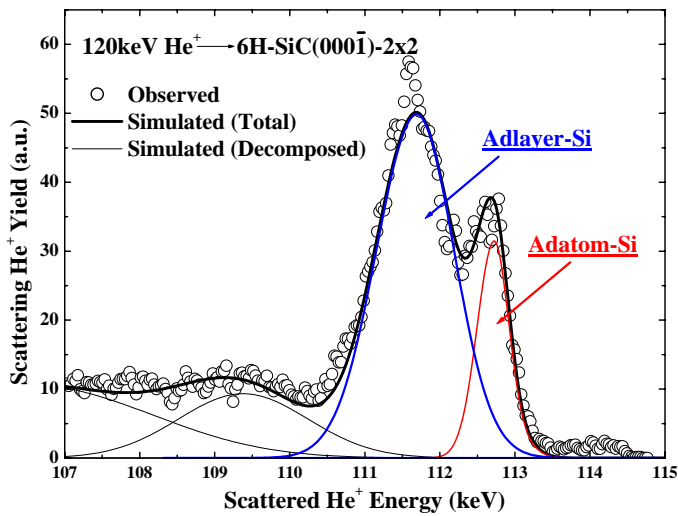


FIG. 2. MEIS spectrum observed for 120 keV He^+ ions incident at incident and detection angles of 54.7° and 88.0° , respectively in the $(1\bar{1}00)$ plane. The bright and deep gray areas correspond to the scattering components from the Si-adatoms and the Si-adlayer, respectively.

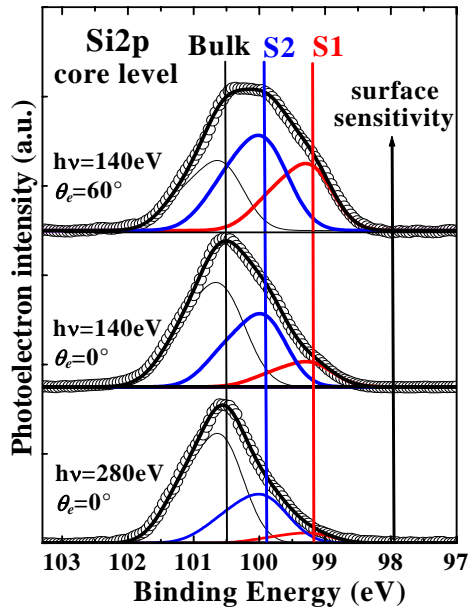


FIG. 3. Si 2p core level spectra observed at photon energy of 140 eV with emission angles of 60° (a) and 0° (b) and at 280 eV with an emission angle of 0° (c). The components of S1 and S2 comes from the Si-adatoms and the Si-adlayer, respectively.

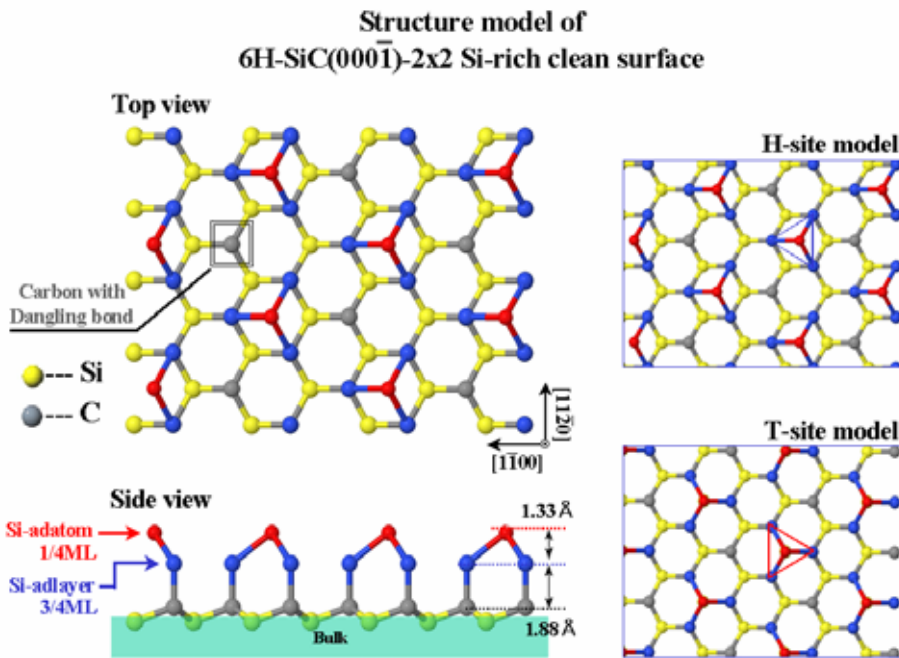


FIG.4. Top and side

views of a probable surface structure for the 6H-SiC(000 $\bar{1}$)-2x2. Open and closed circles denote Si and C atoms, respectively. The larger the circles size, the upper the lattice positions. The Si-adatoms take a T-site (left side) and an H-site (right side). P, Q, R, Q' and R' indicate adlayer atoms common to the two models, although strictly all the atoms are equivalent by C_{3v} symmetry in each model. S indicates the adatom.

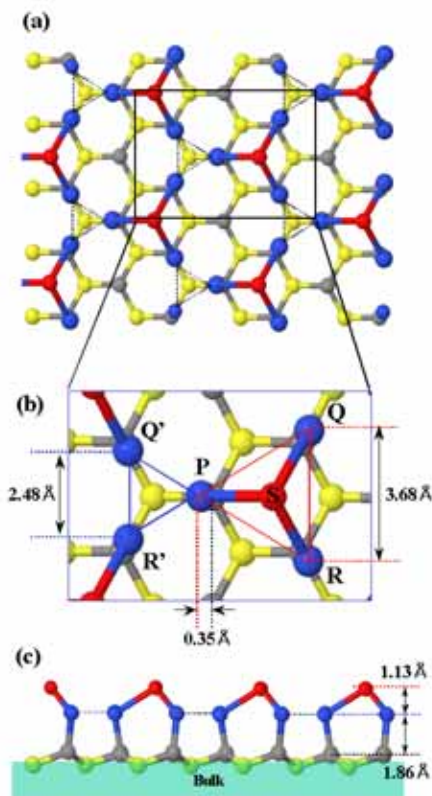


FIG. 5. Top and side views of the surface structure predicted by the *ab initio* calculations. Open and closed circles show Si and C atoms, respectively. P, Q, R, Q' and R' are the adlayer atoms and S indicates the adatom.

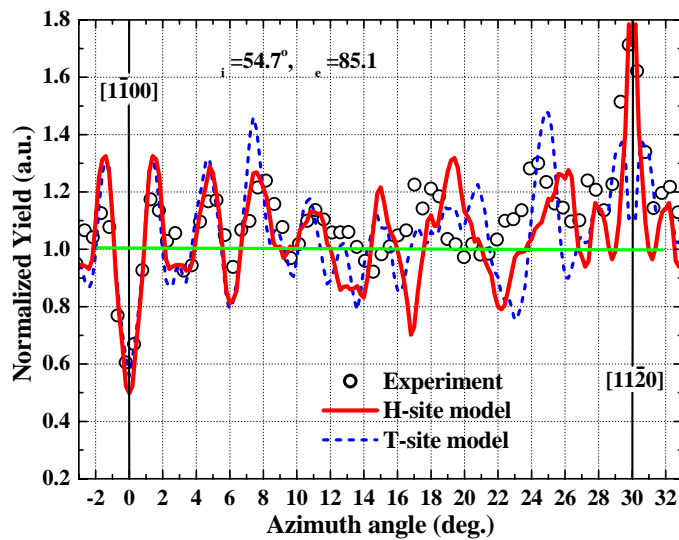


FIG. 6. Azimuth scan profile observed for the scattering component mainly from Si of the top C-Si bilayer (open circles). The incident and detection angles were fixed at 54.7° and 85.1° with respect to surface normal. The azimuth angles of 0° and 30° correspond to the crystal planes of $[1\bar{1}00]$ and $[11\bar{2}0]$, respectively.